Hindawi Publishing Corporation
EURASIP Journal on Image and Video Processing
Volume 2007, Article ID 47345, 11 pages
doi:10.1155/2007/47345

Research Article

Energy-Efficient Transmission of Wavelet-Based Images in Wireless Sensor Networks

Vincent Lecuire, Cristian Duran-Faundez, and Nicolas Krommenacker

Centre de Recherche en Automatique de Nancy (CRAN UMR 7039), Nancy-Université, CNRS, Faculté des Sciences et Techniques, BP 239, 54506 Vandoeuvre lès Nancy Cedex, France

Received 14 August 2006; Revised 15 December 2006; Accepted 22 December 2006

Recommended by James E. Fowler

We propose a self-adaptive image transmission scheme driven by energy efficiency considerations in order to be suitable for wireless sensor networks. It is based on wavelet image transform and semireliable transmission to achieve energy conservation. Wavelet image transform provides data decomposition in multiple levels of resolution, so the image can be divided into packets with different priorities. Semireliable transmission enables priority-based packet discarding by intermediate nodes according to their battery's state-of-charge. Such an image transmission approach provides a graceful tradeoff between the reconstructed images quality and the sensor nodes' lifetime. An analytical study in terms of dissipated energy is performed to compare the self-adaptive image transmission scheme to a fully reliable scheme. Since image processing is computationally intensive and operates on a large data set, the cost of the wavelet image transform is considered in the energy consumption analysis. Results show up to 80% reduction in the energy consumption achieved by our proposal compared to a nonenergy-aware one, with the guarantee for the image quality to be lower-bounded.

1. INTRODUCTION

Thanks to recent advances in microelectronics and wireless communications, it is predicted that wireless sensor networks (WSN) will become ubiquitous in our daily life and they have already been a hot research area for the past couple of years. A wide range of emerging WSN applications, like object detection, surveillance, recognition, localization, and tracking, require vision capabilities. Nowadays, such applications are possible since low-power sensors equipped with a vision component, like "Cyclops" [1] and "ALOHAim" [2], already exist. Although the hardware prerequisites are met, application-aware and energy-efficient algorithms for both the processing and communication of image have to be developed to make vision sensor applications feasible. Most of the work in the literature is devoted to image processing (data extraction, compression, and analysis) [3–7] while the image transmission over WSN [8] is still in an earlier stage of research.

In this paper, we propose a self-adaptive image transmission scheme driven by energy efficiency considerations in order to provide a graceful tradeoff between the energy consumption to transmit the image data and the quality of the played-out image at the receiver side. The self-adaptive image transmission scheme is based on discrete wavelet transform (DWT) and semireliable transmission to achieve energy conservation. DWT allows for image decomposition into separable subbands for multiresolution representation purposes. As a result, image data can be divided into priority levels. In this way, fully reliable data transmission is only required for the lowest resolution level. The remaining data can be handled with a semireliable transmission policy in order to save energy. Nodes located between the image source and the sink can decide to drop some packets in accordance with the packet priority and the batteries' state-of-charge.

We have developed an energy consumption model in order to compare the self-adaptive image transmission scheme with a fully reliable scheme. Since image processing is computationally intensive and operates on a large data set, the cost of the wavelet image transform is considered in the energy consumption analysis. Numerical results show up to 80% reduction in the energy consumption achieved by our proposal compared to a nonenergy-aware scheme, with a guarantee for the image quality to be lower-bounded.

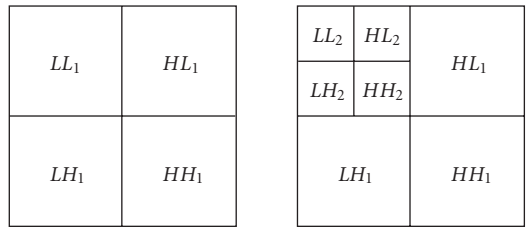

Figure 1: 2D DWT applied once (a) and twice (b).

The remainder of this paper is organized as follows. In Section 2, we describe the technical principles of the self-adaptive image transmission scheme. An analytical study of energy consumption is presented in Section 3. Two strategies for packet prioritization are discussed in Section 4 and numerical results are given in Section 5. Finally, Section 6 concludes and provides some future directions.

2. IMAGE TRANSMISSION PRINCIPLES

The proposed image transmission scheme is based on wavelet image transform and semireliable transmission to achieve the energy conservation. This section describes these technical principles.

2.1. 2D discrete wavelet transform

Discrete wavelet transform [9] is a process which decomposes a signal, that is, a series of digital samples, by passing it through two filters, a lowpass filter L and a highpass filter H. The lowpass subband represents a down-sampled low-resolution version of the original signal. The highpass subband represents residual information of the original signal, needed for the perfect reconstruction of the original set from the low-resolution version.

Since image is typically a two-dimensional signal, a 2D equivalent of the DWT is performed [10]. This is achieved by first applying the L and H filters to the lines of samples, row by row, then refiltering the output to the columns by the same filters. As a result, the image is divided into 4 subbands, LL, LH, HL, and HH, as depicted in Figure 1(a). The LL subband contains the lowpass information and the others contain highpass information of horizontal, vertical and diagonal orientation. The LL subband provides a half-sized version of the input image which can be transformed again to have more levels of resolution. Figure 1(b) shows an image decomposed into three resolution levels.

Generally, an image is partitioned into L resolution levels by applying the 2D DWT $(L-1)$ times. In this way, data packet prioritization can be performed. Packets carrying the image header and the lowest image resolution (represented by the $LL_{(L-1)}$ subband) are the most important, assigned to priority level 0. They have to be reliably received by the sink in order to be able to rebuild a version of the captured image. The data of the other resolutions can be sent with different priorities. In this article, we will discuss in particular two priority policies. The first one assigns priorities according to each level of resolution. In the second one, different priorities are assigned to different coefficient magnitudes obtained in the detail subbands. These policies will be explained in Section 4.

We adopted the Le Gall 5-tap/3-tap wavelet coefficients [11], which was designed explicitly for integer-to-integer transforms in [12]. This wavelet is amenable to energy efficient implementation because it consists of binary shifter and integer adder units rather than multiplier and divisor units. The coefficients of the lowpass filter and of the highpass filter are rational, given by $f_L(z) = -(1/8)\cdot(z^2+z^{-2}) + (1/4)\cdot(z+z^{-1}) + 3/4$ and $f_H(z) = -(1/2)\cdot(z+z^{-1}) + 1$. Then, the output samples are rounded to the nearest integer so that the global amount of data remains the same.

Afterwards, data could be compressed to reduce the global amount of data to send. An entropy coding could be used, such as the Huffman coding which is well known for lossless compression. Entropy coding replaces symbols representation from equal-length to variable-length codes according to their probabilities of occurrence, the most common symbols being linked to the shortest codes. Note that lossy compression techniques could be also used. They achieve a high compression ratio while they are typically more complex and require more computations than the lossless ones. However, traditional compression algorithms are not applicable for current sensor nodes, since they have limited resources, as is discussed in [13]. Basic reasons from this are the algorithm size, processors speed, and memory access. More investigations about efficient compression algorithms in WSN are out of the scope of this paper.

2.2. Semireliable image transmission

Once raw data of the captured image is encoded (applying 2D DWT) and packetized into different priorities, the packets are ready to be sent. The source sensor transmits the packets starting by those with the highest priority, then continues with those of the next lower priority, and so on. Our approach is semireliable in the sense that it is not necessary to transmit all the priority levels to the sink, except the basic one 0. This choice is motivated by the scarce energy in the context of sensor networks. Subsequent priorities are only forwarded if node's battery level is above a given threshold.

In fact, the hop-by-hop transmission is handled as reliable, that is, the data packets are always acknowledged and retransmitted if lost, whereas the end-to-end transmission is handled as semireliable, that is, an intermediate node decides to forward or discard a packet, according to the battery's state-of-charge and the packet's priority. This is carried out using a threshold-based drop scheme where each of the p priorities is associated to an energy level $\alpha_0, \alpha_1, \ldots, \alpha_\ell, \ldots, \alpha_{p-1}$, subject to for all $\ell \in \mathbb{N}$, $\alpha_\ell \in [0,1[$, and $\alpha_\ell < \alpha_{\ell+1}$ (see Figure 2). There remains the question: which values for these

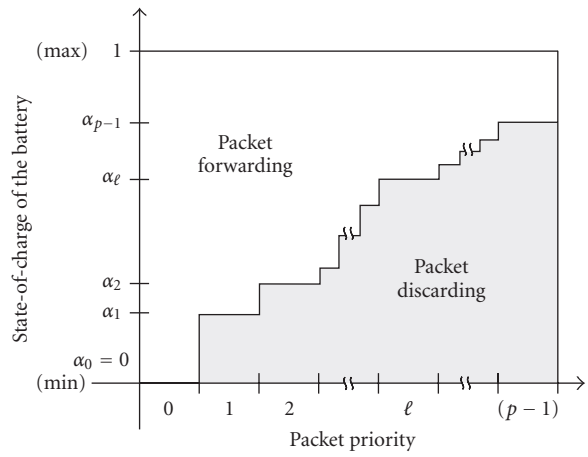

FIGURE 2: Packet forwarding policy based on priorities.

parameters? In practice, this will depend on user application requirements, and it has to be answered prior to the implementation of the protocol.

Of course, the choice of the α_ℓ distribution will influence the results. For instance, if α_ℓ coefficients near 0 are applied, a node adopts a drop scheme which will increase the probability of forwarding packets. Such a policy will promote image quality instead of energy savings. On the contrary, α_ℓ coefficients near 1 will promote energy savings instead of a higher resolution of the final image. This choice will depend on the application in which the WSN is involved.

In this article, our semireliable transmission scheme is qualified as open-loop, because the decision performed by a node is done independently of the available energy in the other nodes. Open-loop transmission presents great adaptation to all type of routing scheme and its modeling and implementation are, certainly, very simple.

We assume that the law of distribution of coefficients α_ℓ is given for each node. When a packet arrives at a node, two pieces of information are needed for the operation to proceed correctly: the priority level assigned to the packet and the total amount of priority levels. This information is provided in the source node and written in the packet header. In the matter, packet header must contain necessarily the following fields: the image identification number, the data offset in the whole image, the total amount of priority levels (p), and the packet priority level (ℓ). An intermediate node will use the third and fourth fields of the packet header to decide whether to discard or forward the received packet. The first and the second fields of the packet header are used by the destination node to store the data in sequence before decoding and playing out the image. The destination node substitutes zero for missing data due to lost packets. As said before, a data packet which is sent to a 1-hop neighbor is immediately acknowledged for transmission error control purposes, even if the receiver decides to discard it. The image transmission scheme is very easy to implement.

2.3. Sink proximity consideration

Until now, we have focused on some energy consumption aspects, leading to the proposal of semireliable transmission scheme. Theoretically, a decrease of the energy consumption could be obtained against the final image resolution. However, when the same energy thresholds are configurated in all nodes of the network, a packet could be discarded by a node that is near the sink, with the same probability that one who is not, even if it has been transmitted through several nodes. Consequently, an efficient packet discarding policy should consider preceding nodes' invested energy. In the matter, the α_ℓ coefficients could evolve based on their sink proximity or, in the same way, in their distance to the source. To this, it is sufficient to use a function of coefficients weighting characterized by $f(1) = 1$ and $\lim_{i\to\infty} f(i) = 0$, where i is the number of accomplished hops from the source. By multiplying the coefficients α_ℓ by the value of $f(i)$ in each intermediate node, the probability of discarding a ℓ resolution packet will decrease while we approach the sink. To implement this proposal, a hop-counter field could be added to the packet header. This hop-counter will be used as input parameter for the function $f(i)$. Now, what function $f(i)$ can we use to make evolve the α_ℓ coefficients while we approach the sink? Answers could be multiple.

Let us analyze a generic function $f(i)$ defined as

$$f_{a,b}(i) = e^{-((i-1)/b)^a}, \tag{1}$$

where a and b (with $a, b > 0$) represent the concavity and stretching factors, respectively. Figure 3 illustrates the effect of each parameter over the function $f_{a,b}(i)$ with a path of 30 intermediate nodes. Both variables a and b define the evolution of the original discarding policy defined by the α_ℓ coefficients. This function is useful due to the adjustments of a and b. The more a increases, the more nodes in the path beginning will respect the original discarding policy (when the packets have crossed a "short distance"); nevertheless, when a greater distance is crossed, the α_ℓ coefficients will decrease drastically (it will be more nodes forwarding almost all packets). For the factor b case, the more it decreases, the more contracted will be the function $f_{a,b}(i)$ (see in Figure 3 the change of $f_{4,15}(i)$ to $f_{4,10}(i)$), and the faster the α_ℓ coefficients will decrease. On the other hand, with greater values of b, $f_{a,b}(i)$ will be more stretched (see in Figure 3 the change of $f_{4,15}(i)$ to $f_{4,20}(i)$), and α_ℓ will diminish more smoothly. If both factors a and b grow up, $f_{a,b}(i)$ function will tend towards the value 1, which means that the same policy will be applied by each node during the whole path.

3. MODELING ENERGY CONSUMPTION

In order to evaluate the benefits of our proposal, we developed a simplified energy consumption model for this self-adaptive image transmission scheme. This model is based on three elementary components: the radio transceiver model, the 2D DWT processing model, and the image transmission model. In order to make the formulas more readable, we

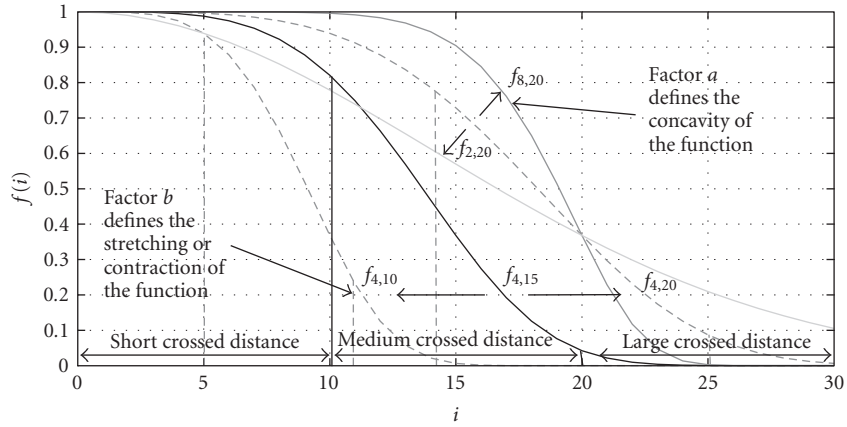

Figure 3: Effect of the stretching and concavity coefficients.

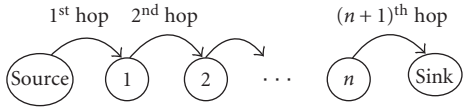

Figure 4: Network path representation.

made, without loss of generality, the following assumptions.

(i) All sensors have the same characteristics.

(ii) The battery state-of-charge of a node does not change significantly during the transmission of a complete image, assuming that the consumed energy per image is not so significant on the scale of a battery capacity and on the network lifetime. As a result, we assume that if the state-of-charge of a node is sufficient to forward a packet for a given priority, then all packets for this priority will be forwarded by this node.

(iii) The network path between the image source and the sink is established by n intermediate nodes numbered from 1 to n in this order (Figure 4). This path is supposed to be steady during the transmission of an image. The 1-hop transmission is assumed to be lossless.

(iv) The image is decomposed into p levels of resolutions.

We wished to evaluate the average amount of dissipated energy to transmit an image throughout the network path from the source to the sink. We determined the number of hops performed by the packets, in relation to their priority levels and the amount of available energy into the different intermediate nodes.

Let $R(\ell, n)$ be the probability that packets with priority ℓ are transmitted to the sink, so $(n+1)$ hops are performed. It means that all the intermediate nodes have enough energy to forward level ℓ packets:

$$R(\ell, n) = \prod_{k=1}^{n} [1 - f(k) \cdot \alpha_\ell] \tag{2}$$

with $0 \le \ell \le p-1$. Let $B(\ell, i)$ be the probability that packets with priority ℓ are dropped before reaching the sink because of the ith node. This corresponds to the probability that node i is the first on the path that does not have enough energy to forward them:

$$B(\ell, i) = \alpha_\ell \cdot f(i) \cdot \prod_{k=1}^{i-1} [1 - f(k) \cdot \alpha_\ell] \tag{3}$$

with $1 \le i \le n$ and $1 \le \ell \le p-1$. Note that $f(i)$ increases the probability of forwarding packets when the node is closer to the sink. Equations (2) and (3) are used to define the energy image transmission model for the open-loop scheme.

3.1. Image transmission energy model

Image data is generally transmitted in more than one packet. So, we introduce m_ℓ as the number of packets required to entirely transmit all packets of priority level ℓ, and t_ℓ as their average size. Let $E(k)$ be the required energy to transmit and acknowledge a k-byte packet between two adjacent nodes (the energy cost per hop). Packets of priority 0 are necessarily transmitted to the sink, then the consumed energy is given by

$$E_{T_0}(m_0, t_0) = (n+1) \cdot m_0 \cdot E(t_0). \tag{4}$$

For other priority levels, associated packets cross at least the first hop. Subsequent hops depend on the amount of energy in the following nodes. The number of hops crossed by packets of priority level ℓ is i if they are dropped at node i; otherwise, it is $(n+1)$. From (2) and (3), the mean consumed energy by the packets of priority level ℓ can be given by

$$E_{T_\ell}(m_\ell, t_\ell) = \underbrace{\sum_{i=1}^{n} B(\ell, i) \cdot i \cdot m_\ell \cdot E(t_\ell)}_{\text{case where the node } i \text{ is blocking}} + \underbrace{R(\ell, n) \cdot (n+1) \cdot m_\ell \cdot E(t_\ell)}_{\text{case where all hops are performed}}. \tag{5}$$

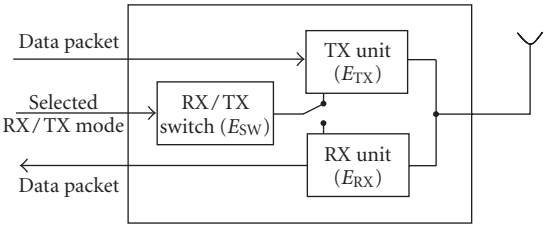

Figure 5: Energy radio transceiver model.

From (4) and (5), the total energy E_T required to transmit the entire image is

$$E_T = (n+1)\cdot m_0 \cdot E(t_0) + \sum_{\ell=1}^{p-1}\left[m_\ell \cdot E(t_\ell)\cdot\left(R(\ell,n)\cdot(n+1)+\sum_{i=1}^{n}B(\ell,i)\cdot i\right)\right]. \quad (6)$$

3.2. Radio transceiver energy model

The transmission of a message between two neighboring nodes requires a set of procedures, each of which consumes a certain amount of energy. Considering that all nodes have the same characteristics, a simple radio transceiver model considers E_{SW}, the consumed energy for mode switching, $E_{TX}(k, P_{out})$, for a k-byte message transmission with a power P_{out}, and $E_{RX}(k)$, for the message reception, as depicted in Figure 5.

With this model, the energy consumed to transmit a k-byte from node i to node j is given by

$$E_{i,j}(k) = 2\cdot E_{SW} + E_{TX}(k, P_{out}) + E_{RX}(k). \quad (7)$$

Considering that the energy is defined in millijoules (mJ), then the energy component can be expressed as the product of voltage, current drawn, and time. So the formula (7) becomes

$$E_{i,j}(k) = k\cdot C_{TX}(P_{out})\cdot V_B\cdot T_{TX} + 2\cdot C_{SW}\cdot V_B\cdot T_{SW} + k\cdot C_{RX}\cdot V_B\cdot T_{RX}, \quad (8)$$

where $C_{TX}(P_{out})$, C_{SW}, and C_{RX} are the current drawn (in mA) by the radio, respectively, in transmission, switching modes, and receiving, T_{TX}, T_{SW}, and T_{RW} are the corresponding operation time (in seconds), and V_B is the typical voltage provided by batteries. As we said in Section 3.1, $E(k)$ is the energy consumed to send a k-byte packet and return the corresponding ACK. If L_{ACK} is the length of the ACK packet, then

$$E(k) = E_{i,j}(k) + E_{j,i}(L_{ACK}). \quad (9)$$

3.3. 2D DWT energy model

An energy consumption model is given by Lee and Dey [14] for 2D discrete wavelet transform based on the integer 5-tap/3-tap wavelet filter. They initially determined the number of times that basic operations are performed in the wavelet image transform as follows: for each sample pixel, lowpass decomposition requires 8 shift and 8 add instructions, whereas highpass decomposition requires 2 shift and 4 adds. Concerning memory accesses, each pixel is read and written twice. Assuming that the input image size is of $M\times N$ pixels and the 2D DWT is iteratively applied T times, then the energy consumption for this process is approximately given by

$$E_{DWT}(M,N,T) = MN\cdot\left(10\varepsilon_{shift}+12\varepsilon_{add}+2\varepsilon_{rmem}+2\varepsilon_{wmem}\right)\cdot\sum_{i=1}^{T}\frac{1}{4^{i-1}}, \quad (10)$$

where ε_{shift}, ε_{add}, ε_{rmem}, and ε_{wmem} represent the energy consumption for shift, add, read, and write basic 1-byte instructions, respectively.

4. STRATEGIES FOR PACKET PRIORITIZATION

In this section, we introduce two possible strategies to assign priorities to data of the detail subbands. The first one is based on resolution levels while the second one is based on wavelet-coefficient magnitudes. Let P_ℓ be the set of packets with priority ℓ. Whatever the priority policy applied, P_0 carries the image header on the lower image resolution. This data is essential to be able to rebuild a version of the image. Other data is classified according to the priority policy chosen. Performance results of both approaches will be discussed later in Section 5.2.

4.1. Priorities based on resolution levels

Such a priority policy is simplest. Assuming that the image is partitioned into L resolution levels, those have a decreasing importance from the resolution 0 to L. The resolution 0 corresponds to $LL_{(L-1)}$ subband (see Figure 1). Other resolutions consist of 3 subbands, the ℓth resolution corresponding to $HL_{L-\ell}$, $LH_{L-\ell}$, and $HH_{L-\ell}$ subbands. With the priority policy based on resolution levels, the data packets carrying the resolution ℓ are, thus, assigned to the priority ℓ.

4.2. Priorities based on coefficient magnitudes

This priority policy considers the importance of data from the wavelet-coefficient magnitudes. Indeed, large-magnitude coefficients have higher importance than small-magnitude coefficients. Consequently, such a priority policy, with p priority levels is carried out using a set of $(p-2)$ magnitude thresholds, $\{\tau_1, \tau_2, \ldots, \tau_{(p-2)}\}$. The priority level of a data packet is assigned as follows: if the packet carries at least one coefficient with an absolute value over a magnitude threshold τ_ℓ, then, the packet will be assigned as of priority ℓ. In formal words, let d_i be the ith value transported by the packet D. If there exists $d_i/|d_i| \geq \tau_\ell$, then $D \in P_\ell$, else, if for all $d_i/|d_i| < \tau_{(p-2)}$, then $D \in P_{(p-1)}$.

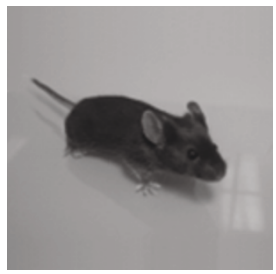

Figure 6: Original test image (128 × 128 pixels).

5. NUMERICAL APPLICATION AND RESULTS

In this section, we apply the energy consumption model to evaluate and compare energy performance of image transmission in various scenarios. For the reasons given in Section 2, we do not consider the image compression. A monochrome image of 128 × 128 pixels, presented in Figure 6, is used as a test image. This one is 8 bits per pixel originally encoded. That means a data length of 16 394 bytes, including the image header of 10 bytes. Numerical values adopted for the input parameters of energy models are described below. Then, we present the results of numerical application.

5.1. Input parameters

5.1.1. Hardware characteristics of sensor nodes

The adopted input parameters refer to the characteristics of Mica2 motes [15]. These devices are based on a low-power 7.37 MHz ATmega128L microcontroller [16], 4 Kbytes EEPROM, a Chipcon CC1000 radio transceiver [17] with FSK modulated radio and an Atmel AT45DB041 serial flash memory [16] with 512 Kbytes for storing data. Typically Mica2 motes work with two AA batteries, able to provide 3 Volts. From technical documentation [18] and some experiences [19–21], we adopted the parameters summarized in Table 1.

From Table 1, we can compute the dissipated energy for transmission (E_{TX}), reception (E_{RX}), switching modes (E_{SW}), and DWT (E_{DWT}) processing per byte. The energy used to transmit and receive (with −20 dBm) is 5.6 μJ per byte and 10.5 μJ per byte, respectively, and to switch modes is 5.3 μJ. Now, from (10), the energy consumed to perform the 2D discrete wavelet transform once is 9.2 μJ per byte. The energy consumption increases by 25% (11.5 μJ per byte) if image wavelet transform is performed twice.

5.1.2. Transmission characteristics of sensor nodes

Mica2 motes run with TinyOS/nesC from UC Berkeley [22]. We used the basic format of multihop message from TinyOS, that reserves 17 bytes for the header and synchronization. The maximum size of a TinyOS data packet is 255 bytes. As mentioned in Section 2.2, image data packets have a header of 4 bytes (the hop-counter mentioned in Section 2.3 is included as part of a multihop message header). Since each image data packet will be encapsulated into a multihop message, the maximum payload length for image data is 234 bytes. Similarly, ACK packet is of 20 bytes (L_{ACK}).

5.2. Performance analysis

5.2.1. Resolution-based strategy

To get a reference, we evaluated the consumed energy by transmitting reliably the whole image (16 394 bytes, including the 10-byte image header) without applying DWT. In the following, we call that the original scenario. The average amount of energy dissipated to transmit the original image is 312.28 mJ per hop. Afterwards, we considered to apply the DWT one and two times. When DWT is applied once, we obtained a P_0 of 4106 bytes (the 10-byte image header are sent as part of P_0) and a P_1 of 12 288 bytes. Similarly, when DWT is applied twice, we obtained 1034, 3072, and 12 288 bytes for P_0, P_1 and P_2, respectively. From (6), we computed the average energy consumption to transmit the image for each scenario. To this, we have used a uniform distribution of coefficients $\alpha_\ell = \ell/p$ and an adaptation function $f_{4,10}(i)$.

Figure 7(a) shows the average consumed energy per hop as a function of the number of intermediate nodes. We notice that the consumed average energy is clearly lower when wavelet transform and semireliable transmission are applied. For instance, considering 30 intermediate nodes, the average energy dissipated to send the image from the source to the sink is of about 98.68 mJ (1-level DWT) and 44.1 mJ (2-level DWT) corresponding to a decrease of 68.4% (1-level DWT) and 85.88% (2-level DWT) of the consumed energy, respectively, compared to the original scenario.

Obviously, semireliable transmission has repercussions on the obtained image's quality. In fact, greater energy savings imply greater degradation of image quality. Figure 8 shows different cases of resulting images. In Figure 8(b), we see the reconstructed image in the best case, that is, 1-level DWT scenario and all data packets have reached the sink. Figures 8(c) and 8(d) show the reconstructed images in the worst cases, that is, for 1- and 2-level DWT scenarios, respectively, and only P_0 received by the sink. These last images could be acceptable, if the requirements of the application define it.

Now, let us define the average PSNR ($\overline{\text{PSNR}}$) as

$$\overline{\text{PSNR}} = R(p-1,n)\cdot \text{PSNR}(p-1) + \sum_{\ell=0}^{p-2} \left([R(\ell,n) - R(\ell+1,n)]\cdot \text{PSNR}(\ell)\right), \tag{11}$$

where PSNR(ℓ) is the calculated PSNR (peak signal-to-noise ratio [23]) of the obtained image with data of resolution levels from P_0 to P_ℓ, only. The PSNR is a ratio commonly used like metric of the quality of an image obtained after some compression or processing. Figure 7(b) shows the variation of the average PSNR for 1- and 2-level DWT scenarios. Considering a path of 30 intermediate nodes, we can see that the obtained average PSNR is about 36.89 dB (1-level DWT) and 31.51 dB (2-level DWT).

Table 1: Parameters for Mica2 motes.

Variables	Description	Value
V_B	Voltage provided by the power source of the ith node	3 V
$C_{TX}(-20)$	Current consumed for the radio of the ith node for sending 1 byte (with −20 dBm)	3.72 mA
C_{RX}	Current consumed for the radio of the ith node for receiving 1 byte	7.03 mA
C_{SW}	Current consumed for the radio of the ith node for switching modes (rx/tx)	7.03 mA
T_{TX}	Time spent for the radio of the ith node for sending 1 byte	4.992E-004 s
T_{RX}	Time spent for the radio of the ith node for receiving 1 byte	4.992E-004 s
T_{SW}	Time spent for the radio of the ith node for switching modes (rx/tx)	250E-6 s
ε_{shift}	Energy consumed for a microcontroller to execute a shift operation over 1 byte	3.3 nJ
ε_{add}	Energy consumed for a microcontroller to execute an addition over 1 byte	3.3 nJ
ε_{rmem}	Energy consumed to read 1 byte from the flash memory	0.26 μJ
ε_{wmem}	Energy consumed to write 1 byte in the flash memory	4.3 μJ

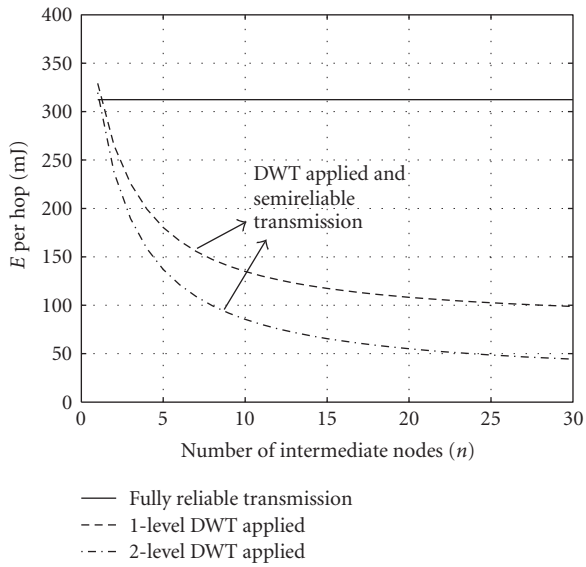

(a) Average energy consumption for semireliable transmission and resolution-based priorities

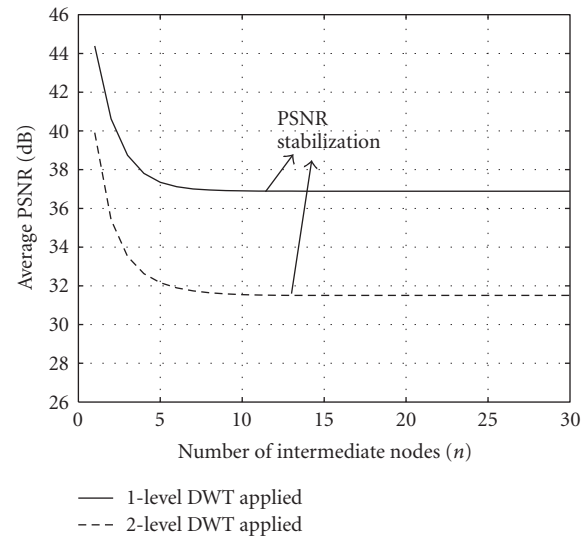

(b) Average PSNR for semireliable transmission and resolution-based priorities

Figure 7: Energy consumption and PSNR for semireliable transmission with uniform distribution in selection of discarding coefficients.

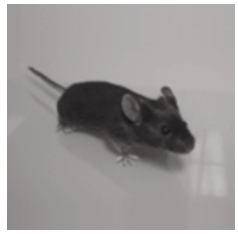

(a) 128 × 128 original image

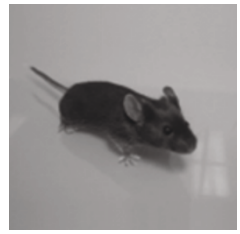

(b) Resulting image with 1 DWT, P_0 + P_1 received (PSNR = 51.91 dB)

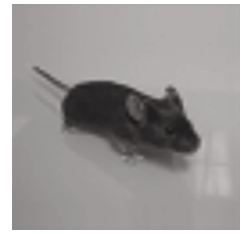

(c) Resulting image with 1 DWT, P_0 received (PSNR = 36.86 dB)

(d) Resulting image with 2 DWT, P_0 received (PSNR = 31.38 dB)

Figure 8: Resulting images with DWT applied.

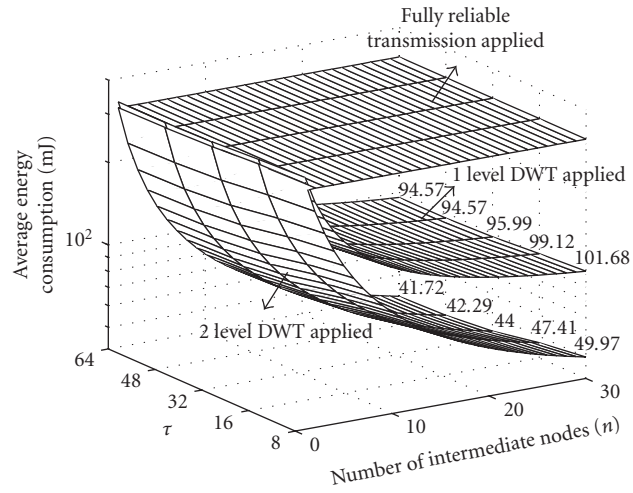

Figure 9: Average energy consumption for semireliable transmission and coefficients magnitudes-based discarding strategy.

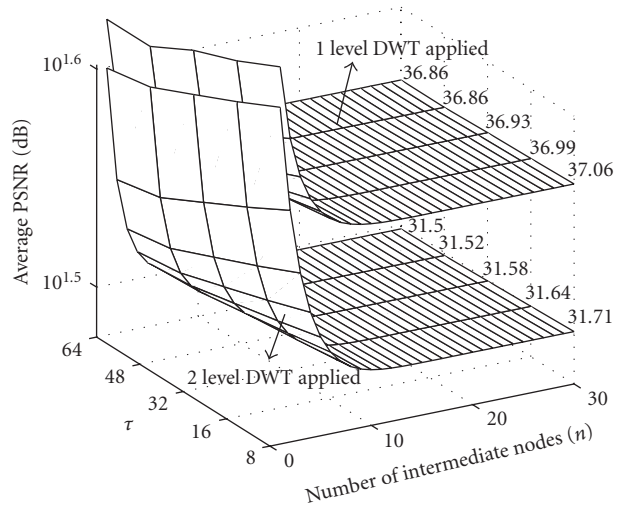

Figure 10: Average PSNR for semireliable transmission and coefficients magnitude-based discarding strategy.

5.2.2. Magnitudes-based strategy

In analogous way to the previous section, we compare the energy consumed in the original scenario with the semireliable transmission scenarios, applying the priority policy based on wavelet-coefficient magnitudes, considering 3 priority levels (i.e., using only 1 magnitude threshold). In order to obtain values for our mathematical model, we performed packet division and prioritization over the test image.

Figure 9 shows the average energy consumption, considering a path of 30 intermediate nodes, and five different values for the magnitude threshold $\tau : \tau = 8$, $\tau = 16$, $\tau = 32$, $\tau = 48$, and $\tau = 64$. We can see that a gain on the energy consumption per hop is obtained with respect to the fully reliable case. With $\tau = 8$, the energy consumption per hop is of 101.68 mJ, corresponding to a decrease of 67.44% compared to the fully reliable case. In Figure 10, we can see that with $\tau = 8$, we obtain an average PSNR of about 37.06 dB. In the other way, when we apply $\tau = 64$ as magnitude threshold, the energy consumption decreases into 84% in comparison with the fully reliable case. Nevertheless, the average PSNR is affected, reaching approximately 36.86 dB, due to the decreasing of the amount of packets to transmit. Consequently, a bigger amount of high coefficients (i.e., useful information for the image reconstruction) is lost. In spite of this, average PSNR continues being largely acceptable.

5.2.3. Comparison of the proposed strategies

In Figure 11(a), we show the average energy consumption of resolution-based strategy versus the magnitudes-based case with three different τ values ($\tau = 8$, $\tau = 32$, and $\tau = 64$). We notice that most of the times magnitudes-based approach gives better PSNR than resolutions-based approach (see Figure 11(b)). However, in some cases, we can obtain better results by applying resolution-based approach, all of this will depend on the chosen magnitude-threshold and on the image content.

To explain this effect, let us take a typical 2-level DWT decomposition of the test image. With the resolution-based strategy applied, we obtain a P_1 (subbands HL_2, LH_2, and HH_2) of 3072 bytes. To transmit this amount of data, a Mica2 mote consumes approximately 58.99 mJ per hop (according to the formula (9)). With the test image, if we receive at the sink P_0 and P_1, and P_2 is lost, we obtain a PSNR of 36.74 dB. In the same way, that is, with the same test image and DWT levels, we obtain a P_1 of 13 packets (3042 bytes of data) with the magnitudes-based strategy, considering $\tau = 32$. In this scenario, we calculated an energy consumption of 57.83 mJ per hop (1.16 mJ less than resolution-based case). By receiving P_0 and P_1 only, we obtained a PSNR of 39.92 dB, 8.66% more than the resolution-based case.

This improvement is obtained because in the resolution-based case we can lose large amount of important data that are in P_2, and we send several packets with coefficients with low significant data. On the other hand, magnitudes-based approach prioritizes highly important data in all the resolutions, before the transmission of low-importance packets. In Figure 12, we can visually notice the differences commented above. We can see that by applying magnitudes-based strategy (Figure 12(c)) we obtain a far better image than if we apply resolution-based strategy (Figure 12(b)).

In the general case, we can conclude that the magnitudes-based strategy is better than the resolution-based strategy.

5.3. Impact of the policy coefficients distribution

We have discussed the impact of the 2D DWT and semireliable transmission application, but we have still not discussed the importance of the α_ℓ coefficients selection. The choice of the coefficients α_ℓ defines the system users priorities. In fact, α_ℓ values near zero imply a tendency towards the image quality, whereas α_ℓ values near one contribute to

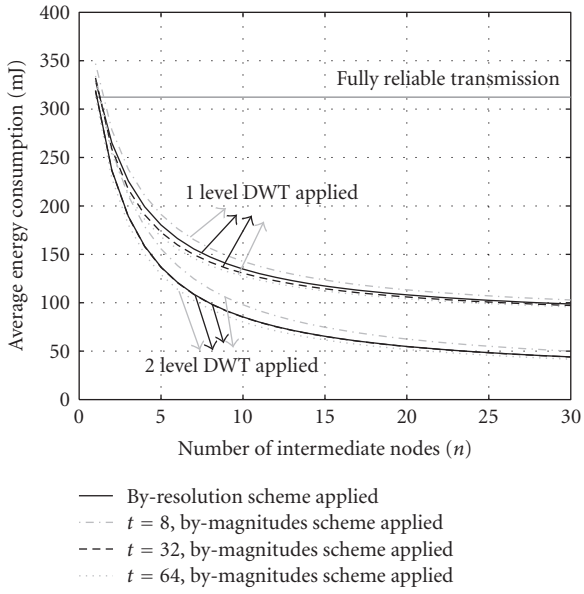

(a) Comparison of average energy consumption for resolutions-based and magnitudes-based priorities and semi-reliable transmission

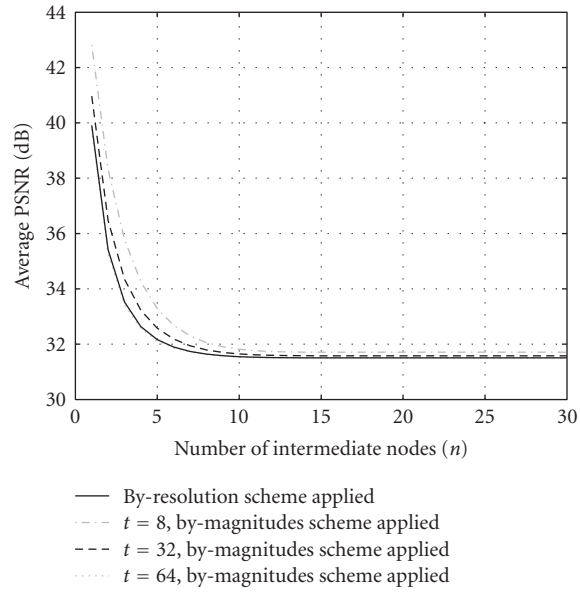

(b) Comparison of average PSNR for resolutions-based and magnitudes-based priorities and semireliable transmission

Figure 11: Comparison of performances for by-resolutions scheme versus by-magnitudes scheme.

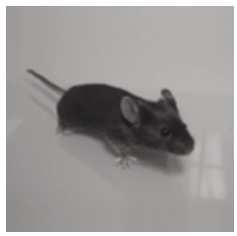

(a) 128 × 128 original image

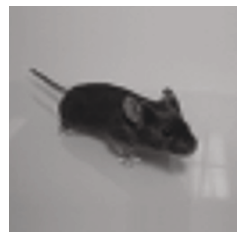

(b) Resulting image with 2 DWT levels, by-resolutions priorities, $P_0 + P_1$ received (PSNR = 36.86 dB)

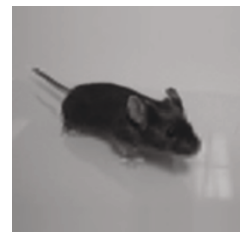

(c) Resulting image with 2 DWT levels, by-magnitudes priorities, $P_0 + P_1$ received (PSNR = 39.92 dB)

Figure 12: Comparison of resulting images by applying different prioritization strategies and packet discarding.

the energy savings. Let us show this statement by applying different α_ℓ in our model.

Graphics in Figure 13 consider α_ℓ values calculated as $\alpha_\ell = (\ell/p)^A$, where A is a factor to define by the user. When $A = 1$, a uniform distribution of α_ℓ coefficients is applied, reflecting no preferences between energy savings and image quality. When $A < 1$, a logarithmic-like distribution is defined in favor of the energy savings. On the other hand, the image quality is prioritized when $A > 1$, defining an exponential-like distribution of the α_ℓ coefficients. In Figure 13, three values of A ($A = 1$, $A = 2/3$, and $A = 3/2$) are used to analyze the impact of different α_ℓ coefficients distribution. Figure 13(a) shows the energy consumption per hop as a function of the network path length: results show up to 85.61% on energy reduction with respect to the non-DWT scenario and $A = 1$. Decreases of 82.05% and 87.03% are obtained by choosing $A = 3/2$ and $A = 2/3$, respectively. Figure 13(b) shows the relationship between average PSNR for 1- and 2-level DWT scenarios and the network path length. We can see that with $A = 3/2$ we obtain the best average image quality, to the detriment of the energy savings.

6. CONCLUSION

In this article, we presented a self-adaptive image transmission protocol for WSNs based in 2D DWT decomposition and semireliable transmission. According to the WSN constraints, this proposal is clearly simple to implement, allowing autonomous and self-adaptive behavior of sensor nodes and providing a compromise between received image

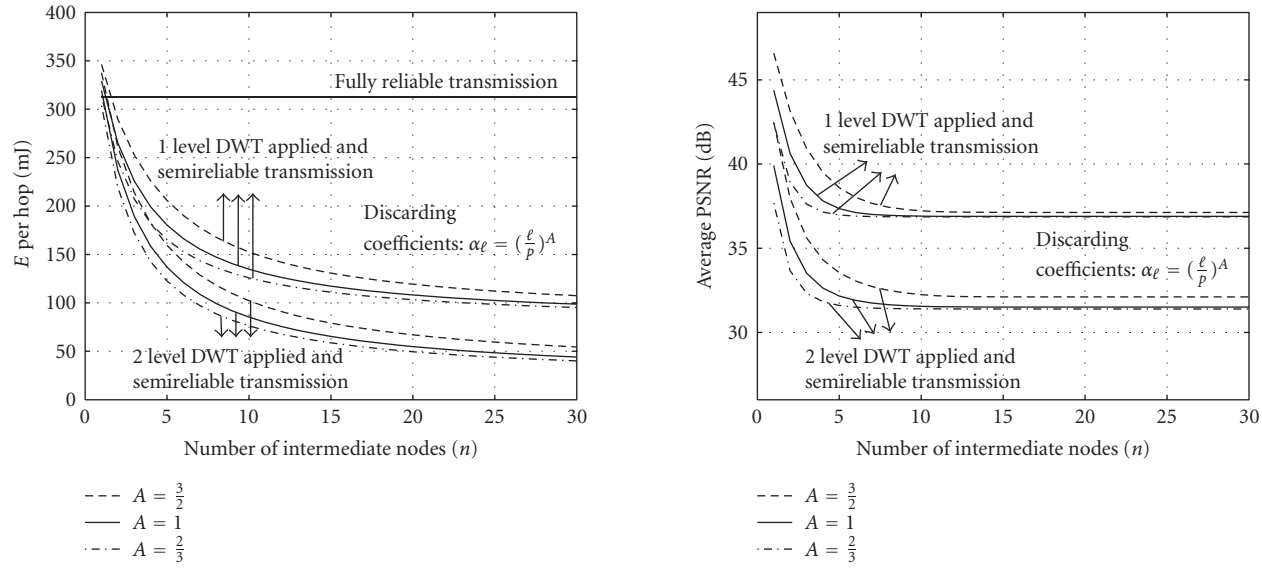

(a) Average energy consumption for 1- and 2-level DWT

(b) Average PSNR for 1- and 2-level DWT applied

Figure 13: Semireliable scheme performance for different distributions on the discarding policy coefficients.

quality and dissipated energy over the network. Two particular strategies for packet prioritization were discussed. The first one considered the prioritization and discarding of packets based on resolution levels. The second one applied a packet prioritization by coefficient magnitudes in detail subbands. We presented these strategies, discussing their characteristics and implementation constraints. We further exposed their performance obtained by applying their parameters in a probabilistic model to measure average energy consumption and average PSNR, obtaining an important reduction of the power consumption with the self-adaptive protocol, in comparison with a traditional fully reliable transmission.

In future works, we will improve our proposal, researching new and better strategies. We will integrate the semireliable transmission protocol with existing routing protocols and multipath algorithms, and we will propose adaptations to improve results. Closed-loop strategies will be investigated, to still improve our proposal. A simulation will be provided to give more complete and real results. Image compression is an important topic that was not considered in the results exposed in this document. Local and distributed compression algorithms will be studied to be incorporated in our proposal, analyzing their performances and their feasibility to be incorporated in a real wireless vision sensor network.

REFERENCES

[1] M. Rahimi, R. Baer, O. I. Iroezi, et al., "Cyclops: in situ image sensing and interpretation in wireless sensor networks," in *Proceedings of the 3rd ACM International Conference on Embedded Networked Sensor Systems (SenSys '05)*, pp. 192–204, San Diego, Calif, USA, November 2005.

[2] E. Culurciello and A. G. Andreou, "CMOS image sensors for sensor networks," *Analog Integrated Circuits and Signal Processing*, vol. 49, no. 1, pp. 39–51, 2006.

[3] E. Magli, M. Mancin, and L. Merello, "Low-complexity video compression for wireless sensor networks," in *Proceedings of International Conference on Multimedia and Expo (ICME '03)*, pp. 585–588, Baltimore, Md, USA, July 2003.

[4] R. Wagner, R. Nowak, and R. Baraniuk, "Distributed image compression for sensor networks using correspondence analysis and super-resolution," in *Proceedings of International Conference on Image Processing (ICIP '03)*, vol. 1, pp. 597–600, Barcelona, Spain, September 2003.

[5] C. Tang and C. S. Raghavendra, "Compression techniques for wireless sensor networks," in *Wireless Sensor Networks*, pp. 207–231, Kluwer Academic, Boston, Mass, USA, 2004.

[6] B. Song, O. Bursalioglu, A. K. Roy-Chowdhury, and E. Tuncel, "Towards a multi-terminal video compression algorithm using epipolar geometry," in *Proceedings of the IEEE International Conference on Acoustics, Speech and Signal Processing (ICASSP '06)*, vol. 2, pp. 49–52, Toulouse, France, May 2006.

[7] H. Wu and A. A. Abouzeid, "Energy efficient distributed image compression in resource-constrained multihop wireless networks," *Computer Communications*, vol. 28, no. 14, pp. 1658–1668, 2005.

[8] H. Wu and A. A. Abouzeid, "Error resilient image transport in wireless sensor networks," *Computer Networks*, vol. 50, no. 15, pp. 2873–2887, 2006.

[9] S. Mallat, *A Wavelet Tour of Signal Processing*, Academic Press, New York, NY, USA, 2nd edition, 1999.

[10] M. Antonini, M. Barlaud, P. Mathieu, and I. Daubechies, "Image coding using wavelet transform," *IEEE Transactions of Image Processing*, vol. 1, no. 2, pp. 205–220, 1992.

[11] D. Le Gall and A. Tabatabai, "Sub-band coding of digital images using symmetric short kernel filters and arithmetic coding techniques," in *Proceedings IEEE International Conference on Acoustics, Speech and Signal Processing (ICASSP '88)*, pp. 761–764, New York, NY, USA, April 1988.

[12] A. R. Calderbank, I. Daubechies, W. Sweldens, and B.-L. Yeo, "Wavelet transforms that map integers to integers," *Applied*

and Computational Harmonic Analysis, vol. 5, no. 3, pp. 332–369, 1998.

[13] N. Kimura and S. Latifi, "A survey on data compression in wireless sensor networks," in *Proceedings of International Conference on Information Technology: Coding and Computing (ITCC '05)*, vol. 2, pp. 8–13, Las Vegas, Nev, USA, April 2005.

[14] D.-G. Lee and S. Dey, "Adaptive and energy efficient wavelet image compression for mobile multimedia data services," in *Proceedings of IEEE International Conference on Communications (ICC '02)*, vol. 4, pp. 2484–2490, New York, NY, USA, April-May 2002.

[15] Crossbow Technology, http://www.xbow.com.

[16] Atmel Corporation, http://www.atmel.com.

[17] Chipcon Products, http://www.chipcon.com.

[18] ATmega128(L) summary. Datasheet, Atmel Corporation, http://www.atmel.com.

[19] V. Shnayder, M. Hempstead, B.-R. Chen, G. W. Allen, and M. Welsh, "Simulating the power consumption of large-scale sensor network applications," in *Proceedings of the 2nd ACM International Conference on Embedded Networked Sensor Systems (SenSys '04)*, pp. 188–200, Baltimore, Md, USA, November 2004.

[20] J. Polastre, J. Hill, and D. Culler, "Versatile low power media access for wireless sensor networks," in *Proceedings of the 2nd ACM International Conference on Embedded Networked Sensor Systems (SenSys '04)*, pp. 95–107, Baltimore, Md, USA, November 2004.

[21] G. Marhur, P. Desnoyers, D. Ganesan, and P. Shenoy, "Ultra-low power data storage for sensor networks," in *Proceedings of IEEE/ACM Conference on Information Processing in Sensor Networks (IPSN '06)*, pp. 374–381, Nashville, Tenn, USA, April 2006.

[22] UC Berkeley, "TinyOS: an operating system for networked sensors," http://www.tinyos.net.

[23] D. Salomon, *Data Compression: The Complete Reference*, Springer, New York, NY, USA, 3rd edition, 2004.